Improved source apportionment of organic aerosols in complex urban air pollution using the multilinear engine (ME-2)

Qiao Zhu[1], Xiao-Feng Huang[1,*], Li-Ming Cao[1], Lin-Tong Wei[1], Bin Zhang[1], Ling-Yan He[1], Miriam Elser[2], Francesco Canonaco[2], Jay G. Slowik[2], Carlo Bozzetti[2], Imad El-Haddad[2], and André S.H. Prévôt[2]

[1]Key Laboratory for Urban Habitat Environmental Science and Technology, School of Environment and Energy, Peking University Shenzhen Graduate School, Shenzhen, 518055, China.

[2]Paul Scherrer Institute (PSI), 5232 Villigen-PSI, Switzerland

Abstract Organic aerosols (OAs), which consist of thousands of complex compounds emitted from various sources, constitute one of the major components of fine particulate matter. The traditional positive matrix factorization (PMF) method often apportions aerosol mass spectrometer (AMS) organic datasets into less meaningful or mixed factors, especially in complex urban cases. In this study, an improved source apportionment method using a bilinear model of the multilinear engine (ME-2) was applied to OAs collected during the heavily polluted season from two Chinese megacities located in the north and south with an Aerodyne high-resolution aerosol mass spectrometer (HR-ToF-AMS). We applied a rather novel procedure for utilization of prior information and selecting optimal solutions, which dose not nessesarily depend on other studies. Ultimately, six reasonable factors were clearly resolved and quantified for both sites by constraining one or more factors: hydrocarbon-like OA (HOA), cooking-related OA (COA), biomass burning OA (BBOA), coal combustion (CCOA), less-oxidized oxygenated OA (LO-OOA) and more-oxidized oxygenated OA (MO-OOA). In comparison, the traditional PMF method could not effectively resolve the appropriate factors, e.g., BBOA and CCOA, in the solutions. Moreover, coal combustion and traffic emissions were determined to be primarily responsible for the concentrations of PAHs and BC, respectively, through the regression analyses of the ME-2 results.

1 Introduction

Atmospheric aerosols are generating increasing interest due to their adverse effects on human health, visibility and the climate (IPCC, 2013; Pope and Dockery, 2006). Among different particulate compositions, many studies focus on organic aerosols (OAs) because they contribute 20-90% to the total submicron mass (Jimenez et al., 2009; Zhang et al., 2007). OAs can be either directly emitted by various sources, including anthropogenic (i.e., traffic and combustion activities) and biogenic sources, or produced via secondary formation after the oxidation of volatile organic compounds (VOCs) (Hallquist et al., 2009).

---

[1] *Correspondence to*: X.-F. Huang (huangxf@pku.edu.cn)

Therefore, the reliable source identification and quantification of OAs are essential before developing effective political abatement strategies.

Aerodyne aerosol mass spectrometer (AMS) systems are the most widely adopted on-line aerosol measurement systems for acquiring aerosol chemical compositions (Canagaratna et al., 2007; Pratt and Prather, 2012). An AMS provides on-line quantitative mass spectra of non-refractory components from the submicron aerosol fraction with a high temporal resolution (i.e., seconds to minutes) (Canagaratna et al., 2007). The total mass spectra can be assigned to both several inorganic compounds and the organic fraction through mass spectral fragmentation tables (Allan et al., 2004). To further investigate the different types of organic fractions, numerous studies have exploited the positive matrix factorization (PMF) algorithm and apportioned the AMS organic mass spectra in terms of their source emissions or formation processes (Zhang et al., 2011). PMF is a standard multivariate factor analysis tool (Paatero, 1999; Paatero and Tapper, 1994) that models the time series of measured organic mass spectra as a linear combination of positive factor profiles and their respective time series. Most of the earlier PMF studies were conducted on unit-mass resolution (UMR) mass spectrometers (Lanz et al., 2007; Lanz et al., 2010; Ulbrich et al., 2009), although more have recently focused on high-resolution (HR) mass spectra PMF (Aiken et al., 2009; Docherty et al., 2008; Huang et al., 2010). The use of HR mass spectra data to constrain PMF solutions can reduce their rotational ambiguity and result in more interpretable OA factors. For example, Aiken et al. (2009) found that hydrocarbon-like OA (HOA) and biomass burning OA (BBOA) were better separated using HR-AMS data than with UMR data. However, even HR-AMS-PMF can also yield mixed factors (especially in heavily polluted areas) due to their complex emission patterns.

The abundant characteristic fragments for cooking-related OA (COA) (e.g., m/z 55 and 57) and coal combustion OA (CCOA) (e.g., m/z 51, 53, and 65) can be observed in the mass spectrum of the HOA factor (He et al., 2010; Hu et al., 2013). Elser (et al., 2016) analyzed two urban HR-AMS datasets in China, and their PMF results showed an HOA profile that contained a high concentration of $C_2H_4O_2^+$ (m/z 60), which is a BBOA tracer ion. In addition, CO_2^+ (m/z 44) contributed more to COA compared to oxygenated OA (OOA). To solve this "mixed factor" problem in PMF analysis, some researchers attempted to use the multilinear engine algorithm (ME-2) with user-provided constraints (Canonaco et al., 2013; Crippa et al., 2014; Elser et al., 2016; Reyes-Villegas et al., 2016). However, several key issues with the ME-2 in these studies, such as reliability of the user-input constraints and the criteria used to determine an optimal result, still require further investigation. Most ME-2 studies (Crippa et al., 2014; Elser et al., 2016; Reyes-Villegas et al., 2016) were based on HR-AMS datasets and utilized mass profiles of PMF results from Paris (Crippa et al., 2013; mostly due to the lack of other reliable source profiles) and did not consider the specific sampling sites, which could result in uncertainties.

In this study, a novel source apportionment technique using the multi-linear engine tool (ME-2) was successfully applied to organic mass spectra obtained with an HR-ToF-AMS at two urban sites during pollution-heavy periods during the same year. The improved OA source apportionment results are discussed and compared with an unconstrained PMF analysis.

2 Materials and methods

2.1 Sampling sites and period

Measurements at Qingdao (36.10°N, 120.47°E, 10 m above ground level, a.g.l.) were performed from 1 to 31 November 2013, while those in Dongguan were conducted from 12 December 2013 to 1 January 2014 (33.03°N, 113.75°E, 100 m a.g.l.). Qingdao is a coastal city with over 9 million inhabitants in northern China, while Dongguan has over 8 million inhabitants and is located in southern China (shown in Figure 1). Both of the sampling sites are on the tops of buildings in urban central areas, and there is no industrial emission nearby.
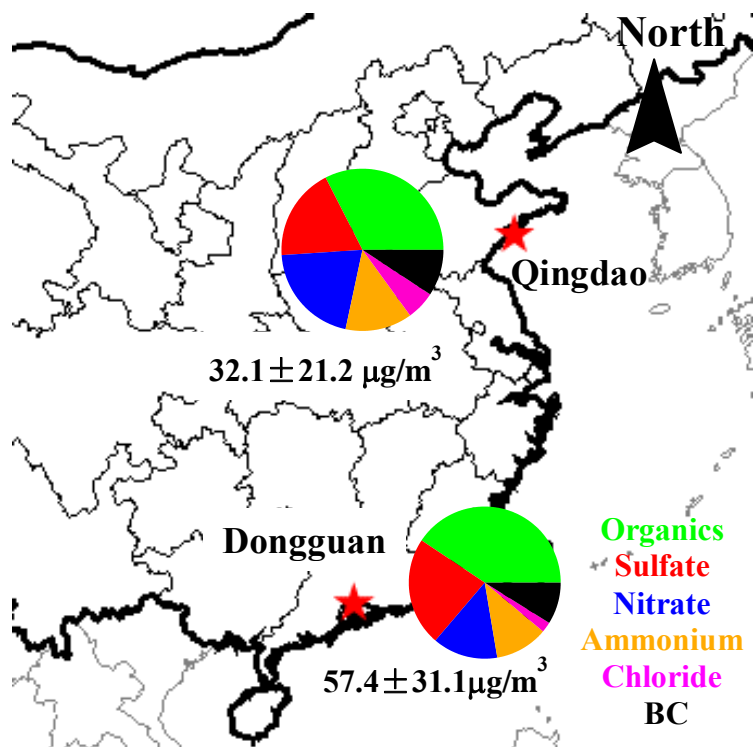
Figure 1. The locations and the average PM_1 chemical compositions of the Qingdao and Dongguan sampling sites.

2.2 Instrumentation

An HR-ToF-AMS was deployed for the on-line measurement of non-refractory PM_1 (Canagaratna et al., 2007). The setup and operation of the HR-ToF-AMS was similar to that in our previous studies (Huang et al., 2015; Huang et al., 2010). A $PM_{2.5}$ cyclone inlet was briefly placed on the roof of a building to remove coarse particles and to introduce an air stream containing the remaining particles into a room through a copper tube with a flow rate of $10 \, l \, min^{-1}$. A nafion dryer (MD-070-12S-4, Perma Pure Inc.) was positioned upstream of the HR–ToF–AMS to eliminate the potential influence of relative humidity on the

particle collection (Matthew et al., 2008), after which the HR–ToF–AMS isokinetically sampled from the center of the copper tube at a flow rate of 80 ml min^{-1}. The instrument was operated at two ion optical modes with a cycle of 4 min, including 2 min for the mass-sensitive V-mode and 2 min for the high mass resolution W-mode. An aethalometer (AE-31, Magee), which also has a PM$_{2.5}$ inlet, was simultaneously used for measurements of refractory black carbon (BC) with a temporal resolution of 5 min.

A routine analysis of the HR–ToF–AMS data was performed using the software SQUIRREL (version 1.57) and PIKA (version 1.16) written in Igor Pro 6.37 (Wave Metrics Inc.)(http://cires1.colorado.edu/jimenezgroup/ToFAMSResources/ToFSoftware / index.html). The ionization efficiency (IE) was calibrated using pure ammonium nitrate particles following standard protocols (Drewnick et al., 2005; Jayne et al., 2000). The relative IEs (RIEs) for organics, nitrate and chloride were assumed to be 1.4, 1.1 and 1.3, respectively. A composition-dependent collection efficiency (CE) was applied to the data based on the method of Middlebrook et al. (2012) and an organic elemental analysis was performed using the latest approach recommended by Canagaratna et al. (2015).

2.3 PMF and ME-2 methods for OA source apportionment

PMF is a mathematical technique used to solve bilinear unmixing problems (Paatero and Tapper, 1994) that enables a description of the variability of a multivariate database as the linear combination of static factor profiles and their corresponding time series. The bilinear factor analytic model in matrix notation is defined in Eq. (1), where the measured matrix X (consisting of i rows and j columns) is approximated by the product of G (containing the factor time series) and F (the factor profiles). E denotes the model residuals. The entries in G and F are fitted using a least-squares algorithm that iteratively minimizes the quantity Q (Eq. 2), which is defined as the sum of the squared residuals (e_{ij}) weighted by their respective uncertainties (σ_{ij}).

$$X = G \times F + E \qquad (1)$$

$$Q = \sum_{i=1}^{m} \sum_{j=1}^{n} \left(\frac{e_{ij}}{\sigma_{ij}} \right)^2 \qquad (2)$$

In this study, we adopted SoFi (Canonaco et al., 2013), which is an implementation of the multilinear engine (ME-2) (Paatero, 1999), to perform the organic HR-AMS data analysis. In contrast to an unconstrained PMF analysis, ME-2 enables a more complete exploration of the rotational ambiguity of the solution space. In our case, this is achieved by directing the solution towards environmentally meaningful rotations using the *a* value approach. This method uses prior input profiles and the scalar a to constrain one or more output factor profiles such that they fall within a predetermined range. The *a* value determines the extent to which the output profiles are allowed to vary from the input profiles according to Eq. (3), where f represents the factor profile and j indicates the *m/z* of the ions.

$$f_{j,solution} = f_j \pm a \times f_j \qquad (3)$$

The number of output factors, which is selected by the user, is a key consideration for PMF analysis. Most unconstrained PMF results were chosen following the procedures detailed in Zhang et al. (2007). However, additional outputs in ME-2 can be

106 generated to explore more of the solution space, and more criteria should be developed to support the factor identification,
107 which will be discussed in section 3.

2.4 Polycyclic aromatic hydrocarbons (PAHs) quantification

109 In this study, PAHs mass concentrations were quantitatively determined from the HR-AMS data. The steps outlined are
110 as follows: first, the PAHs molecular ions [M]$^+$, including [$C_{10}H_8$]$^+$, [$C_{12}H_8$]$^+$, [$C_{14}H_8$]$^+$, [$C_{14}H_{10}$]$^+$, [$C_{16}H_{10}$]$^+$, [$C_{18}H_{10}$]$^+$,
111 [$C_{18}H_{12}$]$^+$, [$C_{20}H_{12}$]$^+$, [$C_{22}H_{12}$]$^+$, [$C_{22}H_{14}$]$^+$, [$C_{24}H_{12}$]$^+$, [$C_{24}H_{14}$]$^+$, and other associated fragments, including [M-H]$^+$, [M-2H]$^+$,
112 [M]$^{2+}$, and [M-H]$^{2+}$ were fitted in the HR spectra. Second, the fragments presented low correlation (i.e., R^2 below 0.6) with
113 their corresponding molecular ions were not taken into account. Finally, the relative ionization efficiencie (RIE) for PAHs was
114 assumed to be 1.4 and the dependency of the collection efficiency (CE_b) on the chemical composition of the aerosol was
115 estimated using a composition-dependent collection efficiency (CDCE) algorithm (Middlebrook et al., 2012). More details
116 about the method can be found in Bruns et al. (2015).

3 Interpretation of OA source apportionment using ME-2

118 In this section, a conventional PMF without any prior information is performed to analyze the OA source apportionment.
119 Then, we use the ME-2 method to optimize the OA source apportionment based on the information obtained from the PMF
120 method. The sequential steps are reported below:

121 1. Unconstrained PMF runs.

122 We performed unconstrained runs with a range from two to ten factors. Generally, PMF solutions with large numbers of
123 factors are not considered due to possible mathematical splits of the factor profiles. However, some factors that have small
124 contributions or that have similar mass profiles as other factors (but different time series) may only be found in solutions with
125 large numbers of factors. We observe that most of the solutions provided via PMF include either multiply split factors or mixed
126 factors that are not properly separated from one another. In other words, PMF does not produce an appropriate solution. The
127 6-factor solutions for Qingdao and Dongguan are shown in Figure S1 and S2, and three types of primary OAs (POAs) were
128 identified for each sampling site, including HOA), coal combustion OA (CCOA) and cooking OA (COA) for Qingdao and
129 HOA, biomass burning OA (BBOA) and COA for Dongguan. Oxygenated OA (OOA) seems to be excessively split in the 6-
130 factor solutions for both of the sites. HOA is distinguished by alkyl fragment signatures with prominent contributions of m/z
131 55 ($C_4H_7^+$) and m/z 57 ($C_4H_9^+$) (Ng et al., 2011). The COA profile is similar to that of HOA but has a higher contribution from
132 oxygenated ions at m/z 55 ($C_3H_3O^+$) and m/z 57 ($C_3H_5O^+$) (Mohr et al., 2012). BBOA is characterized by the presence of
133 signals at m/z 60 ($C_2H_4O_2^+$) and m/z 73 ($C_3H_5O_2^+$), which are identified as fragments from anhydrous sugars present in biomass
134 smoke (Alfarra et al., 2007). The OOA profile is characterized by a high signal at m/z 44 (CO_2^+). Note that some POA profiles
135 in this solution indicate mixing; for example, CCOAs in Qingdao contain a high concentration of the biomass burning tracer
136 ion (m/z 60, $C_2H_4O_2^+$), and HOAs in Dongguan have a higher-than-expected contribution of m/z 44 (CO_2^+) with a high O/C

137   ratio (0.26). In addition, CCOA seems to be mixed with BBOA. We then further verified the solutions with additional factors.

138   The results show that BBOA and CCOA are separated from each other in the 7- and 8-factor solutions for Qingdao (see Figure

139   S1) and that better signals for unmixed and stable HOA with low O/C ratios of 0.17 or 0.18 emerged in the 7- to 10-factor

140   solutions for Dongguan (see Figure S2).

141   2. Investigate anchor profiles for ME-2.

142   Before operating ME-2, feasible and reasonable prior input profiles must be determined. To the best of our knowledge,

143   this is the first HR-OA data set that employs anchor profiles extracted from an unconstrained PMF solution with a higher

144   number of factors, and the same approach has been successfully applied to source apportionment efforts using UMR ME-2

145   (Fröhlich et al., 2015). In our case for Qingdao, the BBOA anchor profile should be investigated, and we attempted to look for

146   it from the unconstrained PMF results based on the same dataset, and found that the BBOA factors in the 7- and 8-factor

147   solutions might be used as the anchor profiles. They both had good correlation with the BBOA MS in Chinese biomass burning

148   emission simulation (He et al., 2010), confirming their basic BBOA characteristics. Although these two BBOA factors are

149   quite similar, the BBOA from the 8-factor solution is better suited to be a constraining profile due to its smaller m/z 44 (CO_2^+)

150   signal and higher m/z 60 ($C_2H_4O_2^+$) signal (see Figure S3). In addition, the BBOA from the 8-factor solution also correlates

151   better with the BBOA from a Chinese biomass burning simulation (R^2=0.81) than the 7-factor solution (R^2=0.79). For

152   Dongguan, the anchor profile for HOA can be obtained from unconstrained PMF solutions. The averaged HOA profile from

153   the 7- to 10-factor solutions was used as the anchor profile for ME-2 due to the small differences among the different solutions.

154   Additionally, the constraining CCOA profile for Dongguan is still under consideration because the mass spectrum of BBOA

155   was found to be very similar to that of CCOA, raising the concern that coal combustion particles might have been incorrectly

156   apportioned to biomass burning sources (Wang et al., 2013). An appropriate CCOA anchor profile could not be obtained due

157   to an increase in the unconstrained PMF factor number (see Figure S2). The best approach is to employ the CCOA profile

158   from Qingdao as the constraining profile for Dongguan in ME-2, as these two campaigns were conducted using the same HR-

159   ToF-AMS in the same year. In addition, the CCOA from Qingdao has a very good correlation (R^2=0.97) with CCOA profiles

160   reported at other Chinese urban sites (Elser et al., 2016) (see Figure S4). Tian et al. (2012) also found that the emission

161   compositions of coal combustion in different regions in China are quite similar. The input profiles for BBOA, HOA and CCOA

162   prior to operating ME-2 are shown in Figure 2.

163
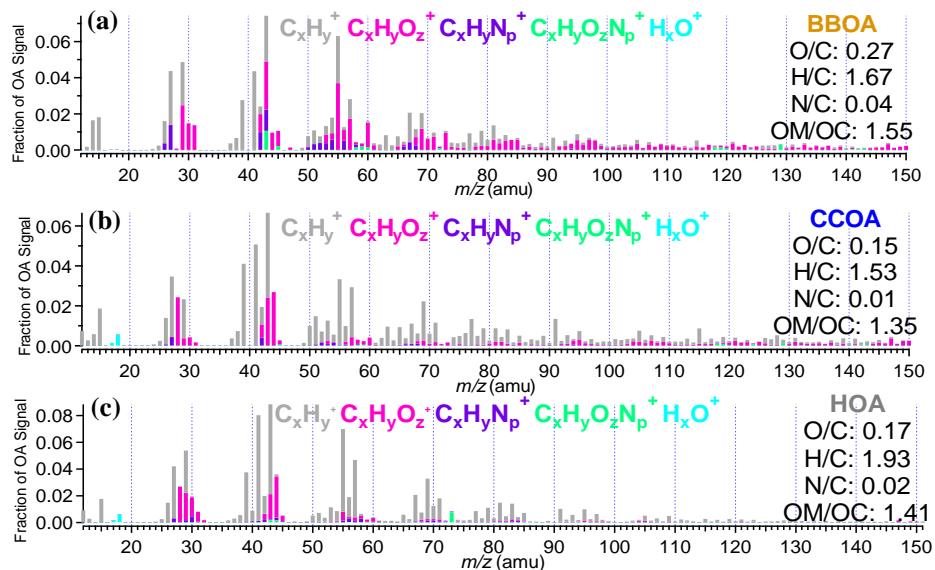
Figure 2. The anchor mass spectra for (a) BBOA, (b) CCOA and (c) HOA in the ME-2 analysis.

3. Constrain the mass spectrums of the mixed factors with different *a* values.

According to the unconstrained PMF results, the best interpretable results for both two sites are the 6-factor solutions with factors that include HOA, COA, BBOA, CCOA, less-oxidized oxygenated OA (LO-OOA) and more-oxidized oxygenated OA (MO-OOA) (Figure 3a and 3b). The *a* values set from 0 to 1 with an increment of 0.1 for BBOA in Qingdao yields 11 possible solutions, and for both HOA and CCOA in Dongguan yields 121 possible solutions.

4. Criteria for obtaining the optimal results.

In this study, we used two simple and reasonable criteria to obtain a better environmental OA source apportionment: the reasonability of the O/C ratio and the correlation between the factors and the tracers. For Qingdao, the O/C ratios for six resolved factors and the correlations between CCOA and PAHs, HOA and BC for 11 solutions with different *a* values are shown in Table S2. These results indicate that all of the O/C ratios for each factor and each factor-tracer correlation are quite similar to one another and that they agree with the range of values in the literature (Canagaratna et al., 2015). Therefore, the solutions averaged over the 11 outputs were considered the final results for Qingdao. For Dongguan, all of the O/C ratios for HOA, CCOA, COA and BBOA among the 121 possible solutions are listed in Table S3. The O/C ratio of HOA in the unconstrained PMF results remained between approximately 0.17 and 0.18, providing a filter criterion with which to assess reasonable ME-2 solutions, and only solutions with *a* values between 0 and 0.1 fell into this range (Table S1). The O/C ratios of other factors for *a* values between 0 and 0.1 are shown in Table S3. The solutions using *a* values between 0 and 0.1 for the HOA profile and an *a* value of 0.9 for the CCOA profile are considered ideal results for three reasons. First, unlike the HOA mass spectra, CCOAs from different sites show higher variability and the CCOA anchor profile is not derived from itself, and therefore, it is reasonable to restrict the constraint with small *a* values for HOA and a looser constraint should be applied for CCOA, which is consistent with the *a* values selecting rules in London ME-2 study (Reyes-Villegas et al., 2016). Second, the

186 POA factors in Dongguan, including HOA and CCOA, have higher O/C ratios likely as a result of a higher atmospheric

187 oxidizing capacity and a stronger photochemical formation in Southern China (Hofzumahaus et al., 2009). Moreover, some

188 studies reported that BBOAs undergo substantial chemical processing immediately after emission and that aged BBOAs had

189 significant concentrations in fresh plumes (Zhou et al., 2017). Thus, CCOAs in Dongguan are very likely to demonstrate

190 relatively higher ages than those in Qingdao (0.15) with higher O/C ratios (but with an O/C ratio of up to 1.25 when the *a*

191 value is 1, which is unacceptable). Third, with an increase in the *a* value for CCOA, two types of OOAs become more

192 distinctive, and the factor correlates better with the tracer (Table S1 and Table S4).

193   In order to prove the improvement of using the anchor profiles generated by the unconstrained PMF run with the same

194 local datasets, we also run the ME-2 analysis using the anchor profiles available in the literature, with the results shown in

195 Table S5 and S6. For Qingdao, the correlations between POAs and their tracers and the Q/Qexp values using the three BBOA

196 profiles in the literature are poorer than using the BBOA obtained in this study (Table S5). For Dongguan, the results from

197 ME-2 using the HOA profiles in the literature are also poorer than using the HOA profiles obtained in this study (Table S6).

198 Therefore, it can be clearly seen that the method to obtain an anchor profile in this study is easier (it does not depend on the

199 results in the literature) and more valid.

200 **4 Results and discussion**

201

202 **4.1 Variations in the OA factors**

203   Figure 1 shows the chemical compounds of PM_1, including the non-refractory (NR) components measured via HR-AMS

204 (i.e., OA, SO_4, NO_3, NH_4 and Cl) and BC concentrations measured via the AE-31, during the sampling period in both Qingdao

205 and Dongguan. The average PM_1 mass concentration was 32.1±21.2 µg/m^3 (mean ± standard deviation) in Qingdao and

206 57.4±31.1 µg/m^3 in Dongguan. The temporal variations in the PM_1 species in conjunction with meteorological parameters are

207 shown in Figure S5. Although Dongguan is located in southern China with relatively less air pollution (Huang et al., 2012),

208 the PM_1 mass concentration was higher. This is mainly because of stagnant meteorological conditions with low average wind

209 speeds (i.e., 2.3 m/s) and a maximum wind speed of less than 6 m/s. Among the PM_1 compounds, OAs accounted for 32.5%

210 of PM_1 in Qingdao and 40.6% in Dongguan. This suggests that OA constitutes a very important fraction at both urban sites.

211 Thus, the final and detailed results of the OA source apportionment are presented in this section.

212 For Qingdao, the final result is the average of all of the ME-2 runs with constraints including *a* values from 0 to 1 fulfilling

213 the criteria described in section 3.2. The mass spectra and time series of the resolved OA sources are shown in Figure 3a. The

214 characteristics of each factor were distinct. The BBOA profile contained the highest *m/z* 60 fraction *f*60 (1.5%) compared to

215 the other factors, and the concentrations were highly correlated with $C_2H_4O_2^+$ (R^2=0.81). The mass spectra of COA was

216 characterized by a high *m/z* 55/57 ratio, which is consistent with previous results (He et al., 2010; Mohr et al., 2012; Sun et al.,

217 2016). In addition, the time series of COA showed a good correlation with its tracer ion $C_6H_{10}O^+$ in accordance with (Sun et

218 al., 2016). HOAs were correlated well with BC (R^2=0.65), and CCOAs were highly correlated with PAHs (R^2=0.94). Among

219 the two types of OOAs, the less-oxidized OOA (LO-OOA) had a lower CO_2^+ fraction and O/C ratio (0.62) compared with the

220 more oxidized OOA (MO-OOA), which had a higher CO_2^+ fraction and O/C (0.91) ratio. The sum of LO-OOA and MO-OOA

221 showed a high correlation with the sum of sulfate and nitrate (R^2=0.76). The POAs (including HOA, COA, BBOA and CCOA)

222 contributed 53.4% to the OA concentration (Figure 3a), which was almost equal to the SOA fraction. In terms of the diurnal

223 trends of the OA factors shown in Figure 3a, they are all partially driven both by PBL dynamics (demonstrating an increased

224 dilution during the daytime and an accumulation of particulate matter overnight) and by the diurnal emission profile. The

225 diurnal trend of HOA showed pronounced peaks during the morning and evening rush hours (8:00-9:00 and 19:00-21:00),

226 which is typically the case for traffic-related pollutants. COA shows a very distinct daily trend with strong peaks during the

227 lunch (approximately 12:00) and dinner (19:00-20:00) periods. CCOAs constituted an important and dominant source of

228 pollutants during the wintertime in northern Chinese areas (Elser et al., 2016) due to heating activities, especially with regard

229 to the central-heating supply that began on November 13 and continued until the end of the campaign. The diurnal variations

230 of the four POA factors before and during the central-heating period are shown in Figure S6. In comparison with the other

231 three POAs, the diurnal pattern of CCOA showed a clear increase during the central-heating period with concentration peaks

232 during the morning (at approximately 9:00) and at night (starting to rise at 18:00), which seems consistent with heating

233 emissions and atmospheric dilution. The diurnal trends of BBOA were similar to those of CCOA. The dilution of these particles

234 within a deeper PBL during the daytime resulted in a decreasing trend in the BBOA concentration, while peaks related to

235 residential heating were observed during the morning (between 09:00 to 10:00) and at night (starting to rise at 17:00). The

236 main difference between the LO-OOA and MO-OOA diurnal patterns is that an increase in the MO-OOA mass concentration

237 was observed during the daytime, implying that the formation of secondary organic aerosols was greatly enhanced during the

238 afternoon. In addition, the diurnal cycle for LO-OOA showed a relatively smaller decrease during the daytime compared with

239 the POA factors. These characteristics of the OOA diurnal trend confirm their secondary nature.

240 For Dongguan, similar to the OA source apportionment using ME-2 in Qingdao, the final result is the average of two

241 accepted a-value solutions with six identified factors, including HOA, CCOA, COA, Aged-BBOA, LO-OOA and MO-OOA.

242 Although the range of the O/C ratio of BBOA reported in Canagaratna et al. (2015) was from 0.25 to 0.55, fresh BBOA was

243 found to be rapidly converted to OOA in less than 1 day (Bougiatioti et al., 2014), and the O/C ratio of aged BBOA could be

244 up to 0.85 (Zheng et al., 2017). BBOA in Dongguan was apparently not fresh considering it is an urban site and Dongguan has

245 a warmer winter (17 ℃ in Dongguan vs. 9 ℃ in Qingdao). The BBOA factor identified in Dongguan, with a strong contribution

246 of m/z 60, had a higher O/C, indicating it was an oxygenated BBOA, therefore we name it Aged-BBOA in this study. All of

247 the information regarding the final source results is shown in Figure 3b. Good correlations between each OA factor and their

248 tracers indicate that the resolved ME-2 results are reasonable. A few sharp drops (which always occurred at approximately

249 20:00) were observed in the MO-OOA time series ranging from December 29 to January 5, which coincides with extreme

250 organic aerosol pollution (Figure S5). The inherent mechanisms for these drops remain unexplained, although we have tried a

number of reasonable approaches (e.g., splitting the period into sub-periods to identify the sources, constraining more factors before running ME-2, and examining more factors) to address this issue. A similar problem in the MO-OOA time series was also found in a recent ME-2 application (Qin et al., 2017). In our case, we presume this might be the result of relatively worse meteorological conditions at night during the sampling period, thereby increasing the contribution of late supper emissions and leading to the overestimation of COAs offset by drops in the MO-OOA concentration. Also note that the O/C ratios of the POAs in Dongguan were higher than those in Qingdao, suggesting that POA emissions in Dongguan underwent faster chemical processing. In addition, the relatively smaller contributions of POAs further support this inference. Freshly emitted POAs may get mixed with aged OAs more easily, while ME-2 may still consider them unmixed. MO-OOAs accounted for an average of 42.8% of the total OA mass (which is much greater than the contribution of LO-OOAs), which is probably because some POA species could have been rapidly converted to very aged OOAs (Bougiatioti et al., 2014; Xu et al., 2015). As mentioned above, the characteristics of the diurnal trends of the POA factors in Dongguan were similar to those in Qingdao, and thus, we focused on the OOA factors. MO-OOAs still showed higher concentrations during the daytime but, unlike LO-OOAs in Qingdao, the diurnal patterns of LO-OOAs in Dongguan were flat, implying that secondary OA formation in the LO-OOAs basically offset the influences of PBL variations.

Meteorological conditions (especially wind) play a crucial role in the dilution and transport of air pollution. We used the relationships between the component concentrations and wind to profoundly understand the origins of the OA factors and their nature. The distributions of the OA factor concentrations versus the wind direction and speed are plotted in Figure S7. For both of the urban sites, higher mass concentrations of the POA factors were mostly accompanied by low wind speeds, denoting their local emission characteristics. Additionally, for the OOA factors, a large proportion of their higher concentrations were maintained at higher wind speeds, indicating that the OOAs were formed by transport processes. However, the small fraction of high-level OOAs that was concentrated within the low wind-speed region represents the fast formation of OOAs from some local POA.

273
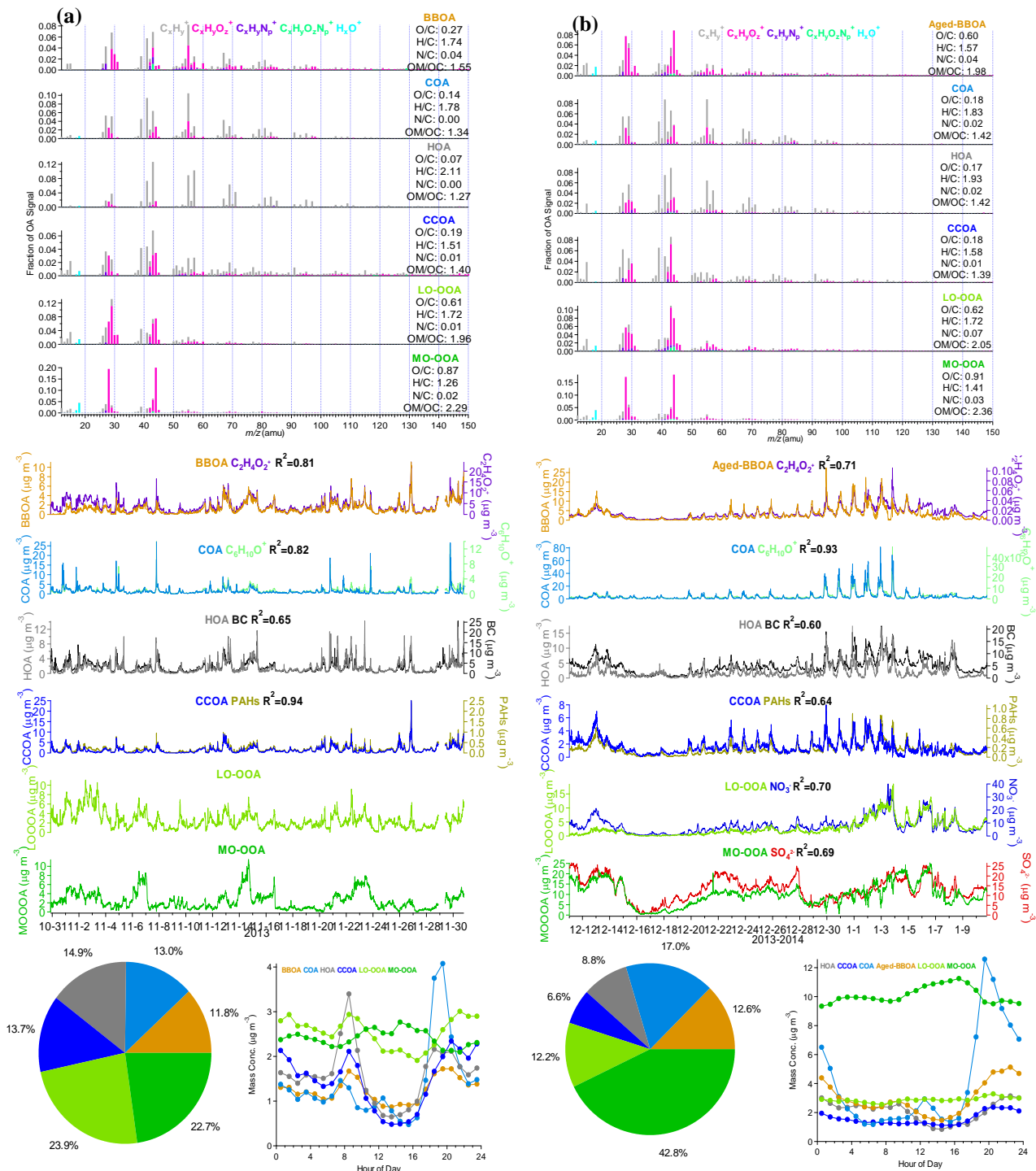
Figure 3. Mass spectra of the OA factors, average fractions of the OA factors, diurnal variations of the OA factors and time series of the OA factors identified by the ME-2 method for (a)Qingdao and (b) Dongguan.

276

4.2 Regression analysis for POA tracers

BC and PAHs are mainly derived from incomplete combustion processes (Schmidt and Noack, 2000; White, 1985), and thus, they were used as tracers for the POAs. In this study, the BC was directly measured by the AE-31, and the PAHs were quantified using the method developed by Bruns et al. (2015) based on AMS data. Both the BC and PAHs showed pronounced diurnal cycles similar to those of the POAs (see Figure S8). In addition, POAs are properly split into different subtypes via the ME-2 method, thereby providing the possibility to better understand the contributions of different POAs to BC and PAHs and to verify the POA source identification. In this section, we use a multi-linear regression method to analyze the POA factors for BC and PAHs.

Figure 4 shows the average contributions of OA sources to BC and PAHs in Qingdao and Dongguan. At both sites, HOAs were the dominant attribute of BC (51% for Qingdao and 40% for Dongguan) and CCOAs contributed the most to the PAHs (59% for Qingdao and 43% for Dongguan), indicating that BC mainly originates from traffic emissions and that PAHs in the Chinese urban polluted atmosphere are dominated by coal combustion during the wintertime. These findings are consistent with results reported in similar studies (Elser et al., 2016; Huang et al., 2015; Huang et al., 2010; Sun et al., 2016; Xu et al., 2014; Zhang et al., 2008). Moreover, the ratio of PAHs to OAs (1.8%) in Qingdao was similar to that in the northern Chinese urban site of Xi'an (1.9%) (Elser et al., 2016) but was higher than that in Dongguan (0.9%). This is likely because a larger fraction of coal combustion to the total OA concentration would enhance the ratio of PAHs to OAs (Elser et al., 2016). Biomass burning was the second-most important source for both BC and PAHs; it was responsible for 33% and 29% of the BC at Qingdao and Dongguan, respectively, and for 29% and 34% of the PAHs at Qingdao and Dongguan, respectively. Cooking emissions were a minor source of BC and PAHs, accounting for less than 10%. These results are also consistent with the published findings. For example, biomass burning is an important source for BC (Kondo et al., 2011; Reddy et al., 2002) and, in some regions with fewer traffic emissions, BC has the best correlation with BBOAs (Schwarz et al., 2008). In addition, in Beijing and California, PAHs are correlated well with BBOAs but are much more weakly correlated with COAs (Ge et al., 2012; Hu et al., 2016; Sun et al., 2016).
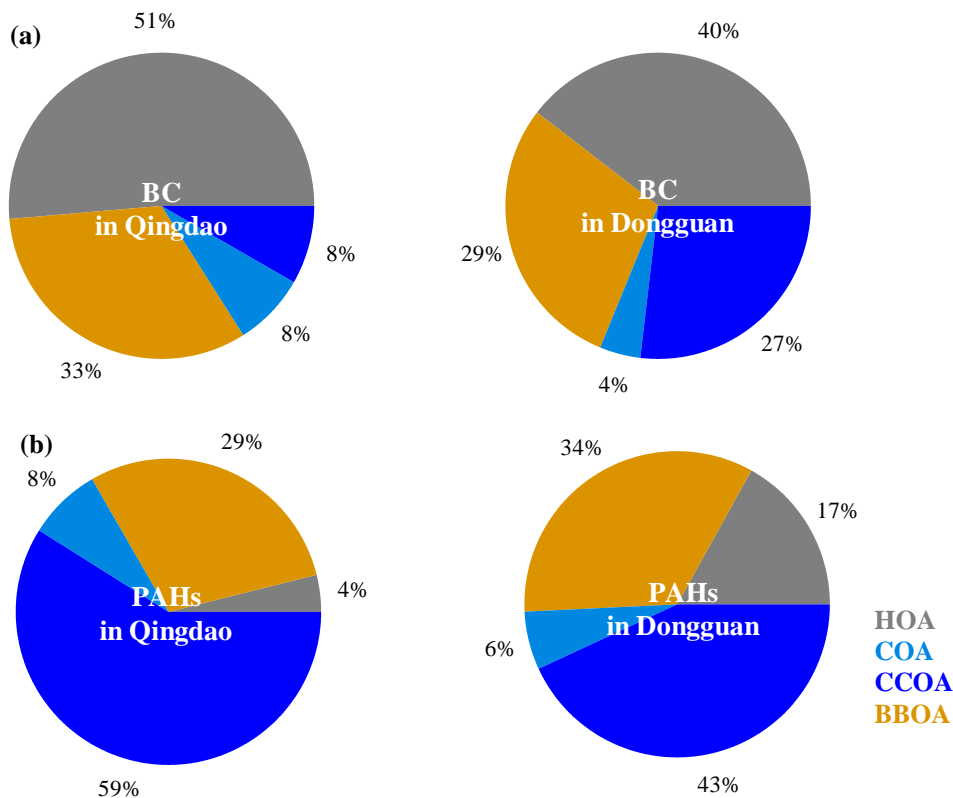
Figure 4. (a) Average contributions of POA factors to BC; (b) average contributions of POA factors to PAHs.

5 Conclusions

In this study, we used PMF to interpret the organic aerosol sources at two Chinese urban sites in winter, and found that PMF did not work properly (i.e., it did not allow for the separation of several primary sources of OAs). Therefore, we adopted the ME-2 approach, which yields more reliable solutions. Technically, there are three important steps when using the ME-2 method to interpret the sources of OAs. The first step is to investigate the mixed and unidentified factors that are constrained according to issues in the unconstrained PMF results. Generally, we constrained one or more POA factors (i.e., HOA, COA, BBOA and CCOA) for the polluted urban sites. The second step is to search for a reasonable anchor profile for each constrained factor. Two approaches were used: searching for anchor profiles via an increase in the number of unconstrained PMF factors from the same data set and using mass profiles derived from other similar studies. The third step is to choose the criteria for obtaining the optimal results. The choice of a reasonable range of O/C ratios may represent a good criterion for HR-OA apportionment since the O/C ratio is a significant and distinctive characteristic for different OA factors. In addition, correlations between the resolved OA factors and their tracers were also suggested.

Acknowledgments

This work was supported by the National Natural Science Foundation of China (91744202, U1301234), the Ministry of Science and Technology of China (2017YFC0210004), and the Science and Technology Plan of Shenzhen Municipality (JCYJ20170412150626172).

References

Aiken, A. C., D. Salcedo, M. J. Cubison, J. A. Huffman, P. F. DeCarlo, I. M. Ulbrich, K. S. Docherty, D. Sueper, J. R. Kimmel, D. R. Worsnop, A. Trimborn, M. Northway, E. A. Stone, J. J. Schauer, R. M. Volkamer, E. Fortner, B. de Foy, J. Wang, A. Laskin, V. Shutthanandan, J. Zheng, R. Zhang, J. Gaffney, N. A. Marley, G. Paredes-Miranda, W. P. Arnott, L. T. Molina, G. Sosa, and J. L. Jimenez : Mexico City aerosol analysis during MILAGRO using high resolution aerosol mass spectrometry at the urban supersite (T0) – Part 1: Fine particle composition and organic source apportionment, Atmos. Chem. Phys., 9(17), 6633-6653, doi: 10.5194/acp-9-6633-2009,2009.

Alfarra, M. R., A. S. H. Prevot, S. Szidat, J. Sandradewi, S. Weimer, V. A. Lanz, D. Schreiber, M. Mohr, and U. Baltensperger : Identification of the Mass Spectral Signature of Organic Aerosols from Wood Burning Emissions, Environ Sci. Technol., 41(16), 5770-5777, doi: 10.1021/es062289b,2007.

Allan, J. D., A. E. Delia, H. Coe, K. N. Bower, M. R. Alfarra, J. L. Jimenez, A. M. Middlebrook, F. Drewnick, T. B. Onasch, M. R. Canagaratna, J. T. Jayne, and D. R. Worsnop: A generalised method for the extraction of chemically resolved mass spectra from Aerodyne aerosol mass spectrometer data, J. Aerosol Sci., 35(7), 909-922, doi: https://doi.org/10.1016/j.jaerosci.2004.02.007,2004.

Bougiatioti, A., I. Stavroulas, E. Kostenidou, P. Zarmpas, C. Theodosi, G. Kouvarakis, F. Canonaco, A. S. H. Prévôt, A. Nenes, S. N. Pandis, and N. Mihalopoulos : Processing of biomass-burning aerosol in the eastern Mediterranean during summertime, Atmos. Chem. Phys., 14(9), 4793-4807, doi: 10.5194/acp-14-4793-2014,2014.

Bruns, E. A., M. Krapf, J. Orasche, Y. Huang, R. Zimmermann, L. Drinovec, G. Močnik, I. El-Haddad, J. G. Slowik, J. Dommen, U. Baltensperger, and A. S. H. Prévôt : Characterization of primary and secondary wood combustion products generated under different burner loads, Atmos. Chem. Phys., 15(5), 2825-2841, doi: 10.5194/acp-15-2825-2015,2015.

Canagaratna, M. R., J. L. Jimenez, J. H. Kroll, Q. Chen, S. H. Kessler, P. Massoli, L. Hildebrandt Ruiz, E. Fortner, L. R. Williams, K. R. Wilson, J. D. Surratt, N. M. Donahue, J. T. Jayne, and D. R. Worsnop : Elemental ratio measurements of organic compounds using aerosol mass spectrometry: characterization, improved calibration, and implications, Atmos. Chem. Phys., 15(1), 253-272, doi: 10.5194/acp-15-253-2015,2015.

Canagaratna, M. R., J. T. Jayne, J. L. Jimenez, J. D. Allan, M. R. Alfarra, Q. Zhang, T. B. Onasch, F. Drewnick, H. Coe, A. Middlebrook, A. Delia, L. R. Williams, A. M. Trimborn, M. J. Northway, P. F. DeCarlo, C. E. Kolb, P. Davidovits, and

344   D. R. Worsnop : Chemical and microphysical characterization of ambient aerosols with the aerodyne aerosol mass
345   spectrometer, Mass Spectrom. Rev., 26(2), 185-222, doi: 10.1002/mas.20115,2007.

346   Canonaco, F., M. Crippa, J. G. Slowik, U. Baltensperger, and A. S. H. Prévôt : SoFi, an IGOR-based interface for the
347   efficient use of the generalized multilinear engine (ME-2) for the source apportionment: ME-2 application to aerosol
348   mass spectrometer data, Atmos. Meas. Tech., 6(12), 3649-3661, doi: 10.5194/amt-6-3649-2013,2013.

349   Crippa, M., DeCarlo, P. F., Slowik, J. G., Mohr, C., Heringa, M.F., Chirico, R., Poulain, L., Freutel, F., Sciare, J., Cozic, J.,
350   DiMarco, C. F., Elsasser, M., José, N., Marchand, N., Abidi, E.,Wiedensohler, A., Drewnick, F., Schneider, J.,
351   Borrmann, S.,Nemitz, E., Zimmermann, R., Jaffrezo, J.-L., Prévôt, A. S. H.,and Baltensperger, U.: Wintertime aerosol
352   chemical compositionand source apportionment of the organic fraction in themetropolitan area of Paris, Atmos. Chem.
353   Phys., 13, 961–981,doi:10.5194/acp-13-961-2013, 2013.

354   Crippa, M., F. Canonaco, V. a. Lanz, M. Äijälä, J. D. Allan, S. Carbone, G. Capes, D. Ceburnis, M. Dall'Osto, D. A. Day, P.
355   F. DeCarlo, M. Ehn, a. Eriksson, E. Freney, L. Hildebrandt Ruiz, R. Hillamo, J. L. Jimenez, H. Junninen, A. Kiendler-
356   Scharr, A. M. Kortelainen, M. Kulmala, A. Laaksonen, A. A. Mensah, C. Mohr, E. Nemitz, C. O'Dowd, J. Ovadnevaite,
357   S. N. Pandis, T. Petäjä, L. Poulain, S. Saarikoski, K. Sellegri, E. Swietlicki, P. Tiitta, D. R. Worsnop, U. Baltensperger,
358   and A. S. H. Prévôt: Organic aerosol components derived from 25 AMS data sets across Europe using a consistent ME-2
359   based source apportionment approach, Atmos. Chem. Phys., 14(12),6159-6176, doi: 10.5194/acp-14-6159-2014, 2014.

360   Docherty, K. S., E. A. Stone, I. M. Ulbrich, P. F. DeCarlo, D. C. Snyder, J. J. Schauer, R. E. Peltier, R. J. Weber, S. M.
361   Murphy, J. H. Seinfeld, B. D. Grover, D. J. Eatough, and J. L. Jimenez : Apportionment of Primary and Secondary
362   Organic Aerosols in Southern California during the 2005 Study of Organic Aerosols in Riverside (SOAR-1), Environ
363   Sci. Technol., 42(20), 7655-7662, doi: 10.1021/es8008166,2008.

364   Drewnick, F., S. S. Hings, P. DeCarlo, J. T. Jayne, M. Gonin, K. Fuhrer, S. Weimer, J. L. Jimenez, K. L. Demerjian, S.
365   Borrmann, and D. R. Worsnop : A New Time-of-Flight Aerosol Mass Spectrometer (TOF-AMS)—Instrument
366   Description and First Field Deployment, Aerosol Sci. Tech., 39(7), 637-658, doi: 10.1080/02786820500182040,2005.

367   Elser, M., R. J. Huang, R. Wolf, J. G. Slowik, Q. Wang, F. Canonaco, G. Li, C. Bozzetti, K. R. Daellenbach, Y. Huang, R.
368   Zhang, Z. Li, J. Cao, U. Baltensperger, I. El-Haddad, and A. S. H. Prévôt : New insights into PM2.5 chemical
369   composition and sources in two major cities in China during extreme haze events using aerosol mass spectrometry,
370   Atmos. Chem. Phys., 16(5), 3207-3225, doi: 10.5194/acp-16-3207-2016,2016.

371   Fröhlich, R., V. Crenn, A. Setyan, C. A. Belis, F. Canonaco, O. Favez, V. Riffault, J. G. Slowik, W. Aas, M. Aijälä, A.
372   Alastuey, B. Artiñano, N. Bonnaire, C. Bozzetti, M. Bressi, C. Carbone, E. Coz, P. L. Croteau, M. J. Cubison, J. K.
373   Esser-Gietl, D. C. Green, V. Gros, L. Heikkinen, H. Herrmann, J. T. Jayne, C. R. Lunder, M. C. Minguillón, G. Močnik,
374   C. D. O'Dowd, J. Ovadnevaite, E. Petralia, L. Poulain, M. Priestman, A. Ripoll, R. Sarda-Estève, A. Wiedensohler, U.
375   Baltensperger, J. Sciare, and A. S. H. Prévôt : ACTRIS ACSM intercomparison – Part 2: Intercomparison of ME-2
376   organic source apportionment results from 15 individual, co-located aerosol mass spectrometers, Atmos. Meas. Tech.,
377   8(6), 2555-2576, doi: 10.5194/amt-8-2555-2015,2015.

Ge, X., A. Setyan, Y. Sun, and Q. Zhang : Primary and secondary organic aerosols in Fresno, California during wintertime: Results from high resolution aerosol mass spectrometry, J. Geophys. Res.-Atmos., 117(D19), 161-169, doi: 10.1029/2012JD018026,2012.

Hallquist, M., J. C. Wenger, U. Baltensperger, Y. Rudich, D. Simpson, M. Claeys, J. Dommen, N. M. Donahue, C. George, A. H. Goldstein, J. F. Hamilton, H. Herrmann, T. Hoffmann, Y. Iinuma, M. Jang, M. E. Jenkin, J. L. Jimenez, A. Kiendler-Scharr, W. Maenhaut, G. McFiggans, T. F. Mentel, A. Monod, A. S. H. Prévôt, J. H. Seinfeld, J. D. Surratt, R. Szmigielski, and J. Wildt : The formation, properties and impact of secondary organic aerosol: current and emerging issues, Atmos. Chem. Phys., 9(14), 5155-5236, doi: 10.5194/acp-9-5155-2009,2009.

He, L. Y., Y. Lin, X. F. Huang, S. Guo, L. Xue, Q. Su, M. Hu, S. J. Luan, and Y. H. Zhang : Characterization of high-resolution aerosol mass spectra of primary organic aerosol emissions from Chinese cooking and biomass burning, Atmos. Chem. Phys., 10(23), 11535-11543, doi: 10.5194/acp-10-11535-2010,2010.

Hofzumahaus, A., F. Rohrer, K. Lu, B. Bohn, T. Brauers, C.-C. Chang, H. Fuchs, F. Holland, K. Kita, Y. Kondo, X. Li, S. Lou, M. Shao, L. Zeng, A. Wahner, and Y. Zhang : Amplified Trace Gas Removal in the Troposphere, Science, 324(5935), 1702, doi: 10.1126/science.1164566,2009.

Hu, W., M. Hu, W. Hu, J. L. Jimenez, B. Yuan, W. Chen, M. Wang, Y. Wu, C. Chen, Z. Wang, J. Peng, L. Zeng, and M. Shao : Chemical composition, sources, and aging process of submicron aerosols in Beijing: Contrast between summer and winter, J. Geophys. Res.-Atmos., 121(4), 1955-1977, doi: 10.1002/2015JD024020,2016.

Hu, W. W., M. Hu, B. Yuan, J. L. Jimenez, Q. Tang, J. F. Peng, W. Hu, M. Shao, M. Wang, L. M. Zeng, Y. S. Wu, Z. H. Gong, X. F. Huang, and L. Y. He: Insights on organic aerosol aging and the influence of coal combustion at a regional receptor site of central eastern China, Atmos. Chem. Phys., 13(19), 10095-10112, doi: 10.5194/acp-13-10095-2013,2013.

Huang, R. J., Y. Zhang, C. Bozzetti, K. F. Ho, J. J. Cao, Y. Han, K. R. Daellenbach, J. G. Slowik, S. M. Platt, F. Canonaco, P. Zotter, R. Wolf, S. M. Pieber, E. A. Bruns, M. Crippa, G. Ciarelli, A. Piazzalunga, M. Schwikowski, G. Abbaszade, J. Schnelle-Kreis, R. Zimmermann, Z. An, S. Szidat, U. Baltensperger, I. El Haddad, and A. S. H. Prévôt: High secondary aerosol contribution to particulate pollution during haze events in China, Nature, 514(7521), 218-222, doi: 10.1038/nature13774,2015.

Huang, X. F., L. Y. He, L. Xue, T. L. Sun, L. W. Zeng, Z. H. Gong, M. Hu, and T. Zhu: Highly time-resolved chemical characterization of atmospheric fine particles during 2010 Shanghai World Expo, Atmos. Chem. Phys., 12(11), 4897-4907, doi: 10.5194/acp-12-4897-2012,2012.

Huang, X. F., L. Y. He, M. Hu, M. R. Canagaratna, Y. Sun, Q. Zhang, T. Zhu, L. Xue, L. W. Zeng, X. G. Liu, Y. H. Zhang, J. T. Jayne, N. L. Ng, and D. R. Worsnop : Highly time-resolved chemical characterization of atmospheric submicron particles during 2008 Beijing Olympic Games using an Aerodyne High-Resolution Aerosol Mass Spectrometer, Atmos. Chem. Phys., 10(18), 8933-8945, doi: 10.5194/acp-10-8933-2010,2010.

410 IPCC , Climate Change 2013: The Physical Science Basis. Contribution of Working Group I to the Fifth Assessment Report

411   of the Intergovernmental Panel on Climate Change, 1535 pp., Cambridge University Press, Cambridge, United Kingdom

412   and New York, NY, USA,2013.

413 Jayne, J. T., D. C. Leard, X. Zhang, P. Davidovits, K. A. Smith, C. E. Kolb, and D. R. Worsnop: Development of an Aerosol

414   Mass Spectrometer for Size and Composition Analysis of Submicron Particles, Aerosol Sci. Tech., 33(1-2), 49-70, doi:

415   10.1080/027868200410840,2000.

416 Jimenez, J. L., M. R. Canagaratna, N. M. Donahue, A. S. H. Prevot, Q. Zhang, J. H. Kroll, P. F. DeCarlo, J. D. Allan, H.

417   Coe, N. L. Ng, A. C. Aiken, K. S. Docherty, I. M. Ulbrich, A. P. Grieshop, A. L. Robinson, J. Duplissy, J. D. Smith, K.

418   R. Wilson, V. A. Lanz, C. Hueglin, Y. L. Sun, J. Tian, A. Laaksonen, T. Raatikainen, J. Rautiainen, P. Vaattovaara, M.

419   Ehn, M. Kulmala, J. M. Tomlinson, D. R. Collins, M. J. Cubison, J. Dunlea, J. A. Huffman, T. B. Onasch, M. R. Alfarra,

420   P. I. Williams, K. Bower, Y. Kondo, J. Schneider, F. Drewnick, S. Borrmann, S. Weimer, K. Demerjian, D. Salcedo, L.

421   Cottrell, R. Griffin, A. Takami, T. Miyoshi, S. Hatakeyama, A. Shimono, J. Y. Sun, Y. M. Zhang, K. Dzepina, J. R.

422   Kimmel, D. Sueper, J. T. Jayne, S. C. Herndon, A. M. Trimborn, L. R. Williams, E. C. Wood, A. M. Middlebrook, C. E.

423   Kolb, U. Baltensperger, and D. R. Worsnop : Evolution of Organic Aerosols in the Atmosphere, Science, 326(5959),

424   1525-1529, doi: 10.1126/science.1180353,2009.

425 Kondo, Y., H. Matsui, N. Moteki, L. Sahu, N. Takegawa, M. Kajino, Y. Zhao, M. J. Cubison, J. L. Jimenez, S. Vay, G. S.

426   Diskin, B. Anderson, A. Wisthaler, T. Mikoviny, H. E. Fuelberg, D. R. Blake, G. Huey, A. J. Weinheimer, D. J. Knapp,

427   and W. H. Brune:Emissions of black carbon, organic, and inorganic aerosols from biomass burning in North America

428   and Asia in 2008, J. Geophys. Res.-Atmos., 116(D8), 353-366, doi: 10.1029/2010JD015152,2011.

429 Lanz, V. A., M. R. Alfarra, U. Baltensperger, B. Buchmann, C. Hueglin, and A. S. H. Prévôt : Source apportionment of

430   submicron organic aerosols at an urban site by factor analytical modelling of aerosol mass spectra, Atmos. Chem. Phys.,

431   7(6), 1503-1522, doi: 10.5194/acp-7-1503-2007,2007.

432 Lanz, V. A., A. S. H. Prévôt, M. R. Alfarra, S. Weimer, C. Mohr, P. F. DeCarlo, M. F. D. Gianini, C. Hueglin, J. Schneider,

433   O. Favez, B. D'Anna, C. George, and U. Baltensperger: Characterization of aerosol chemical composition with aerosol

434   mass spectrometry in Central Europe: an overview, Atmos. Chem. Phys., 10(21), 10453-10471, doi: 10.5194/acp-10-

435   10453-2010,2010.

436 Matthew, B. M., A. M. Middlebrook, and T. B. Onasch : Collection Efficiencies in an Aerodyne Aerosol Mass Spectrometer

437   as a Function of Particle Phase for Laboratory Generated Aerosols, Aerosol Sci. Tech., 42(11), 884-898, doi:

438   10.1080/02786820802356797,2008.

439 Middlebrook, A. M., R. Bahreini, J. L. Jimenez, and M. R. Canagaratna : Evaluation of Composition-Dependent Collection

440   Efficiencies for the Aerodyne Aerosol Mass Spectrometer using Field Data, Aerosol Sci. Tech., 46(3), 258-271, doi:

441   10.1080/02786826.2011.620041,2012.

442 Mohr, C., P. F. DeCarlo, M. F. Heringa, R. Chirico, J. G. Slowik, R. Richter, C. Reche, A. Alastuey, X. Querol, R. Seco, J.

443   Peñuelas, J. L. Jiménez, M. Crippa, R. Zimmermann, U. Baltensperger, and A. S. H. Prévôt : Identification and

444   quantification of organic aerosol from cooking and other sources in Barcelona using aerosol mass spectrometer data,

445   Atmos. Chem. Phys., 12(4), 1649-1665, doi: 10.5194/acp-12-1649-2012,2012.

446   Ng, N. L., M. R. Canagaratna, J. L. Jimenez, Q. Zhang, I. M. Ulbrich, and D. R. Worsnop : Real-Time Methods for

447   Estimating Organic Component Mass Concentrations from Aerosol Mass Spectrometer Data, Environ Sci. Technol.,

448   45(3), 910-916, doi: 10.1021/es102951k,2011.

449   Paatero, P. :The Multilinear Engine: A Table-Driven, Least Squares Program for Solving Multilinear Problems, including

450   the n-Way Parallel Factor Analysis Model, J. Comput. Graph. Stat., 8(4), 854-888, doi: 10.2307/1390831,1999.

451   Paatero, P., and U. Tapper : Positive matrix factorization: A non-negative factor model with optimal utilization of error

452   estimates of data values, Environmetrics, 5(2), 111-126, doi: 10.1002/env.3170050203,1994.

453   Pope, C. A., and D. W. Dockery : Health Effects of Fine Particulate Air Pollution: Lines that Connect, J. Air Waste

454   Manage.,56(6), 709-742, doi: 10.1080/10473289.2006.10464485,2006.

455   Pratt, K. A., and K. A. Prather : Mass spectrometry of atmospheric aerosols—Recent developments and applications. Part II:

456   On-line mass spectrometry techniques, Mass Spectrom. Rev., 31(1), 17-48, doi: 10.1002/mas.20330,2012.

457   Qin, Y. M., H. B. Tan, Y. J. Li, M. I. Schurman, F. Li, F. Canonaco, A. S. H. Prévôt, and C. K. Chan : Impacts of traffic

458   emissions on atmospheric particulate nitrate and organics at a downwind site on the periphery of Guangzhou, China,

459   Atmos. Chem. Phys., 17(17), 10245-10258, doi: 10.5194/acp-17-10245-2017,2017.

460   Reddy, C. M., A. Pearson, L. Xu, A. P. McNichol, B. A. Benner, S. A. Wise, G. A. Klouda, L. A. Currie, and T. I.

461   Eglinton :Radiocarbon as a Tool To Apportion the Sources of Polycyclic Aromatic Hydrocarbons and Black Carbon in

462   Environmental Samples, Environ Sci. Technol., 36(8), 1774-1782, doi: 10.1021/es011343f,2002.

463   Reyes-Villegas, E., D. C. Green, M. Priestman, F. Canonaco, H. Coe, A. S. H. Prévôt, and J. D. Allan: Organic aerosol

464   source apportionment in London 2013 with ME-2: exploring the solution space with annual and seasonal analysis,

465   Atmos. Chem. Phys., 16(24), 15545-15559, doi: 10.5194/acp-16-15545-2016,2016.

466   Schmidt, M. W. I., and A. G. Noack : Black carbon in soils and sediments: Analysis, distribution, implications, and current

467   challenges, Global Biogeochem. Cy., 14(3), 777-793, doi: 10.1029/1999GB001208,2000.

468   Schwarz, J. P., R. S. Gao, J. R. Spackman, L. A. Watts, D. S. Thomson, D. W. Fahey, T. B. Ryerson, J. Peischl, J. S.

469   Holloway, M. Trainer, G. J. Frost, T. Baynard, D. A. Lack, J. A. de Gouw, C. Warneke, and L. A. Del

470   Negro :Measurement of the mixing state, mass, and optical size of individual black carbon particles in urban and biomass

471   burning emissions, Geophys Res. Lett., 35(13), L13810, doi: 10.1029/2008GL033968,2008.

472   Sun, Y., W. Du, P. Fu, Q. Wang, J. Li, X. Ge, Q. Zhang, C. Zhu, L. Ren, W. Xu, J. Zhao, T. Han, D. R. Worsnop, and Z.

473   Wang : Primary and secondary aerosols in Beijing in winter: sources, variations and processes, Atmos. Chem. Phys.,

474   16(13), 8309-8329, doi: 10.5194/acp-16-8309-2016,2016.

475   Tian, H., Cheng, K., Wang, Y., Zhao, D., Lu, L., Jia, W. and Hao, J.: Temporal and spatial variation characteristics of

476   atmospheric emissions of Cd, Cr, and Pb from coal in China. Atmospheric Environment, 50: 157-163,doi:

477   10.1016/j.atmosenv.2011.12.045,2012.

478 Ulbrich, I. M., M. R. Canagaratna, Q. Zhang, D. R. Worsnop, and J. L. Jimenez : Interpretation of organic components from
479   Positive Matrix Factorization of aerosol mass spectrometric data, Atmos. Chem. Phys., 9(9), 2891-2918, doi:
480   10.5194/acp-9-2891-2009,2009.

481 Wang, X., B. J. Williams, X. Wang, Y. Tang, Y. Huang, L. Kong, X. Yang, and P. Biswas: Characterization of organic
482   aerosol produced during pulverized coal combustion in a drop tube furnace, Atmos. Chem. Phys., 13(21), 10919-10932,
483   doi: 10.5194/acp-13-10919-2013,2013.

484 White, H. :Black carbon in the environment, J. Wiley,1985.

485 Xu, J., Q. Zhang, M. Chen, X. Ge, J. Ren, and D. Qin: Chemical composition, sources, and processes of urban aerosols
486   during summertime in northwest China: insights from high-resolution aerosol mass spectrometry, Atmos. Chem. Phys.,
487   14(23), 12593-12611, doi: 10.5194/acp-14-12593-2014,2014.

488 Xu, L., S. Suresh, H. Guo, R. J. Weber, and N. L. Ng : Aerosol characterization over the southeastern United States using
489   high-resolution aerosol mass spectrometry: spatial and seasonal variation of aerosol composition and sources with a
490   focus on organic nitrates, Atmos. Chem. Phys., 15(13), 7307-7336, doi: 10.5194/acp-15-7307-2015,2015.

491 Zhang, Q., J. L. Jimenez, M. R. Canagaratna, I. M. Ulbrich, N. L. Ng, D. R. Worsnop, and Y. Sun : Understanding
492   atmospheric organic aerosols via factor analysis of aerosol mass spectrometry: a review, Anal. Bioanal. Chem., 401(10),
493   3045-3067, doi: 10.1007/s00216-011-5355-y,2011.

494 Zhang, Q., J. L. Jimenez, M. R. Canagaratna, J. D. Allan, H. Coe, I. Ulbrich, M. R. Alfarra, A. Takami, A. M. Middlebrook,
495   Y. L. Sun, K. Dzepina, E. Dunlea, K. Docherty, P. F. DeCarlo, D. Salcedo, T. Onasch, J. T. Jayne, T. Miyoshi, A.
496   Shimono, S. Hatakeyama, N. Takegawa, Y. Kondo, J. Schneider, F. Drewnick, S. Borrmann, S. Weimer, K. Demerjian,
497   P. Williams, K. Bower, R. Bahreini, L. Cottrell, R. J. Griffin, J. Rautiainen, J. Y. Sun, Y. M. Zhang, and D. R.
498   Worsnop :Ubiquity and dominance of oxygenated species in organic aerosols in anthropogenically-influenced Northern
499   Hemisphere midlatitudes, Geophys. Res. Lett., 34(13), L13801, doi: 10.1029/2007GL029979,2007.

500 Zhang, Y., J. J. Schauer, Y. Zhang, L. Zeng, Y. Wei, Y. Liu, and M. Shao : Characteristics of Particulate Carbon Emissions
501   from Real-World Chinese Coal Combustion, Environ Sci. Technol., 42(14), 5068-5073, doi: 10.1021/es7022576,2008.

502 Zhou, S., S. Collier, D. A. Jaffe, N. L. Briggs, J. Hee, A. J. Sedlacek Iii, L. Kleinman, T. B. Onasch, and Q. Zhang :
503   Regional influence of wildfires on aerosol chemistry in the western US and insights into atmospheric aging of biomass
504   burning organic aerosol, Atmos. Chem. Phys., 17(3), 2477-2493, doi: 10.5194/acp-17-2477-2017,2017.

505